

Search for the associated production of a b quark and a neutral supersymmetric Higgs boson which decays to tau pairs

V.M. Abazov³⁷, B. Abbott⁷⁵, M. Abolins⁶⁵, B.S. Acharya³⁰, M. Adams⁵¹, T. Adams⁴⁹, E. Aguilo⁶, M. Ahsan⁵⁹, G.D. Alexeev³⁷, G. Alkhazov⁴¹, A. Alton^{64,a}, G. Alverson⁶³, G.A. Alves², L.S. Ancu³⁶, M. Aoki⁵⁰, Y. Arnaud¹⁴, M. Arov⁶⁰, A. Askew⁴⁹, B. Åsman⁴², O. Atramentov^{49,b}, C. Avila⁸, J. BackusMayes⁸², F. Badaud¹³, L. Bagby⁵⁰, B. Baldin⁵⁰, D.V. Bandurin⁵⁹, S. Banerjee³⁰, E. Barberis⁶³, A.-F. Barfuss¹⁵, P. Baringer⁵⁸, J. Barreto², J.F. Bartlett⁵⁰, U. Bassler¹⁸, D. Bauer⁴⁴, S. Beale⁶, A. Bean⁵⁸, M. Begalli³, M. Begel⁷³, C. Belanger-Champagne⁴², L. Bellantoni⁵⁰, J.A. Benitez⁶⁵, S.B. Beri²⁸, G. Bernardi¹⁷, R. Bernhard²³, I. Bertram⁴³, M. Besançon¹⁸, R. Beuselinck⁴⁴, V.A. Bezzubov⁴⁰, P.C. Bhat⁵⁰, V. Bhatnagar²⁸, G. Blazey⁵², S. Blessing⁴⁹, K. Bloom⁶⁷, A. Boehnlein⁵⁰, D. Boline⁶², T.A. Bolton⁵⁹, E.E. Boos³⁹, G. Borisso⁴³, T. Bose⁶², A. Brandt⁷⁸, R. Brock⁶⁵, G. Brooijmans⁷⁰, A. Bross⁵⁰, D. Brown¹⁹, X.B. Bu⁷, D. Buchholz⁵³, M. Buehler⁸¹, V. Buescher²⁵, V. Bunichev³⁹, S. Burdin^{43,c}, T.H. Burnett⁸², C.P. Buszello⁴⁴, P. Calfayan²⁶, B. Calpas¹⁵, S. Calvet¹⁶, E. Camacho-Pérez³⁴, J. Cammin⁷¹, M.A. Carrasco-Lizarraga³⁴, E. Carrera⁴⁹, W. Carvalho³, B.C.K. Casey⁵⁰, H. Castilla-Valdez³⁴, S. Chakrabarti⁷², D. Chakraborty⁵², K.M. Chan⁵⁵, A. Chandra⁵⁴, E. Cheu⁴⁶, S. Chevalier-Théry¹⁸, D.K. Cho⁶², S.W. Cho³², S. Choi³³, B. Choudhary²⁹, T. Christoudias⁴⁴, S. Cihangir⁵⁰, D. Claes⁶⁷, J. Clutter⁵⁸, M. Cooke⁵⁰, W.E. Cooper⁵⁰, M. Corcoran⁸⁰, F. Couderc¹⁸, M.-C. Cousinou¹⁵, D. Cutts⁷⁷, M. Ćwiok³¹, A. Das⁴⁶, G. Davies⁴⁴, K. De⁷⁸, S.J. de Jong³⁶, E. De La Cruz-Burelo³⁴, K. DeVaughan⁶⁷, F. Déliot¹⁸, M. Demarteau⁵⁰, R. Demina⁷¹, D. Denisov⁵⁰, S.P. Denisov⁴⁰, S. Desai⁵⁰, H.T. Diehl⁵⁰, M. Diesburg⁵⁰, A. Dominguez⁶⁷, T. Dorland⁸², A. Dubey²⁹, L.V. Dudko³⁹, L. Duflot¹⁶, D. Duggan⁴⁹, A. Duperrin¹⁵, S. Dutt²⁸, A. Dyshkant⁵², M. Eads⁶⁷, D. Edmunds⁶⁵, J. Ellison⁴⁸, V.D. Elvira⁵⁰, Y. Enari¹⁷, S. Eno⁶¹, H. Evans⁵⁴, A. Evdokimov⁷³, V.N. Evdokimov⁴⁰, G. Facini⁶³, A.V. Ferapontov⁷⁷, T. Ferbel^{61,71}, F. Fiedler²⁵, F. Filthaut³⁶, W. Fisher⁵⁰, H.E. Fisk⁵⁰, M. Fortner⁵², H. Fox⁴³, S. Fuess⁵⁰, T. Gadfort⁷⁰, C.F. Galea³⁶, A. Garcia-Bellido⁷¹, V. Gavrilov³⁸, P. Gay¹³, W. Geist¹⁹, W. Geng^{15,65}, D. Gerbaudo⁶⁸, C.E. Gerber⁵¹, Y. Gershtein^{49,b}, D. Gillberg⁶, G. Ginther^{50,71}, G. Golovanov³⁷, B. Gómez⁸, A. Goussiou⁸², P.D. Grannis⁷², S. Greder¹⁹, H. Greenlee⁵⁰, Z.D. Greenwood⁶⁰, E.M. Gregores⁴, G. Grenier²⁰, Ph. Gris¹³, J.-F. Grivaz¹⁶, A. Grohsjean¹⁸, S. Grünendahl⁵⁰, M.W. Grünewald³¹, F. Guo⁷², J. Guo⁷², G. Gutierrez⁵⁰, P. Gutierrez⁷⁵, A. Haas^{70,d}, P. Haefner²⁶, S. Hagopian⁴⁹, J. Haley⁶³, I. Hall⁶⁵, R.E. Hall⁴⁷, L. Han⁷, K. Harder⁴⁵, A. Harel⁷¹, J.M. Hauptman⁵⁷, J. Hays⁴⁴, T. Hebbeker²¹, D. Hedin⁵², J.G. Hegeman³⁵, A.P. Heinson⁴⁸, U. Heintz⁶², C. Hensel²⁴, I. Heredia-De La Cruz³⁴, K. Herner⁶⁴, G. Hesketh⁶³, M.D. Hildreth⁵⁵, R. Hirosky⁸¹, T. Hoang⁴⁹, J.D. Hobbs⁷², B. Hoeneisen¹², M. Hohlfeld²⁵, S. Hossain⁷⁵, P. Houben³⁵, Y. Hu⁷², Z. Hubacek¹⁰, N. Huske¹⁷, V. Hynek¹⁰, I. Iashvili⁶⁹, R. Illingworth⁵⁰, A.S. Ito⁵⁰, S. Jabeen⁶², M. Jaffré¹⁶, S. Jain⁷⁵, K. Jakobs²³, D. Jamin¹⁵, R. Jesik⁴⁴, K. Johns⁴⁶, C. Johnson⁷⁰, M. Johnson⁵⁰, D. Johnston⁶⁷, A. Jonckheere⁵⁰, P. Jonsson⁴⁴, A. Juste⁵⁰, E. Kajfasz¹⁵, D. Karmanov³⁹, P.A. Kasper⁵⁰, I. Katsanos⁶⁷, V. Kaushik⁷⁸, R. Kehoe⁷⁹, S. Kermiche¹⁵, N. Khalatyan⁵⁰, A. Khanov⁷⁶, A. Kharchilava⁶⁹, Y.N. Khazdheev³⁷, D. Khatidze⁷⁷, M.H. Kirby⁵³, M. Kirsch²¹, J.M. Kohli²⁸, A.V. Kozelov⁴⁰, J. Kraus⁶⁵, A. Kumar⁶⁹, A. Kupco¹¹, T. Kurča²⁰, V.A. Kuzmin³⁹, J. Kvita⁹, F. Lacroix¹³, D. Lam⁵⁵, S. Lammers⁵⁴, G. Landsberg⁷⁷, P. Lebrun²⁰, H.S. Lee³², W.M. Lee⁵⁰, A. Leflat³⁹, J. Lellouch¹⁷, L. Li⁴⁸, Q.Z. Li⁵⁰, S.M. Lietti⁵, J.K. Lim³², D. Lincoln⁵⁰, J. Linnemann⁶⁵, V.V. Lipaev⁴⁰, R. Lipton⁵⁰, Y. Liu⁷, Z. Liu⁶, A. Lobodenko⁴¹, M. Lokajicek¹¹, P. Love⁴³, H.J. Lubatti⁸², R. Luna-Garcia^{34,e}, A.L. Lyon⁵⁰, A.K.A. Maciel², D. Mackin⁸⁰, P. Mättig²⁷, R. Magaña-Villalba³⁴, P.K. Mal⁴⁶, S. Malik⁶⁷, V.L. Malyshev³⁷, Y. Maravin⁵⁹, B. Martin¹⁴, J. Martínez-Ortega³⁴, R. McCarthy⁷², C.L. McGivern⁵⁸, M.M. Meijer³⁶, A. Melnitchouk⁶⁶, L. Mendoza⁸, D. Menezes⁵², P.G. Mercadante⁴, M. Merkin³⁹, A. Meyer²¹, J. Meyer²⁴, N.K. Mondal³⁰, R.W. Moore⁶, T. Moulik⁵⁸, G.S. Muanza¹⁵, M. Mulhearn⁸¹, O. Mundal²², L. Mundim³, E. Nagy¹⁵, M. Naimuddin²⁹, M. Narain⁷⁷, R. Nayyar²⁹, H.A. Neal⁶⁴, J.P. Negret⁸, P. Neustroev⁴¹, H. Nilsen²³, H. Nogima³, S.F. Novaes⁵, T. Nunnemann²⁶, G. Odrant⁴¹, D. Onoprienko⁵⁹, J. Orduna³⁴, N. Osman⁴⁴, J. Osta⁵⁵, R. Otec¹⁰, G.J. Otero y Garzón¹, M. Owen⁴⁵, M. Padilla⁴⁸, P. Padley⁸⁰, M. Pangilinan⁷⁷, N. Parashar⁵⁶, V. Parihar⁶², S.-J. Park²⁴, S.K. Park³², J. Parsons⁷⁰, R. Partridge⁷⁷, N. Parua⁵⁴, A. Patwa⁷³, B. Penning⁵⁰, M. Perfilov³⁹, K. Peters⁴⁵, Y. Peters⁴⁵, P. Pétrouff¹⁶, R. Piegai¹, J. Piper⁶⁵, M.-A. Pleier⁷³, P.L.M. Podesta-Lerma^{34,f}, V.M. Podstavkov⁵⁰, Y. Pogorelov⁵⁵, M.-E. Pol², P. Polozov³⁸, A.V. Popov⁴⁰, M. Prewitt⁸⁰, S. Protopopescu⁷³, J. Qian⁶⁴, A. Quadt²⁴, B. Quinn⁶⁶, M.S. Rangel¹⁶, K. Ranjan²⁹, P.N. Ratoff⁴³, I. Razumov⁴⁰, P. Renkel⁷⁹, P. Rich⁴⁵, M. Rijssenbeek⁷², I. Ripp-Baudot¹⁹, F. Rizatdinova⁷⁶, S. Robinson⁴⁴, M. Rominsky⁷⁵, C. Royon¹⁸, P. Rubinov⁵⁰,

R. Ruchti⁵⁵, G. Safronov³⁸, G. Sajot¹⁴, A. Sánchez-Hernández³⁴, M.P. Sanders²⁶, B. Sanghi⁵⁰, G. Savage⁵⁰, L. Sawyer⁶⁰, T. Scanlon⁴⁴, D. Schaile²⁶, R.D. Schamberger⁷², Y. Scheglov⁴¹, H. Schellman⁵³, T. Schliephake²⁷, S. Schlobohm⁸², C. Schwanenberger⁴⁵, R. Schwienhorst⁶⁵, J. Sekaric⁵⁸, H. Severini⁷⁵, E. Shabalina²⁴, M. Shamim⁵⁹, V. Shary¹⁸, A.A. Shchukin⁴⁰, R.K. Shivpuri²⁹, V. Simak¹⁰, V. Sirotenko⁵⁰, P. Skubic⁷⁵, P. Slattery⁷¹, D. Smirnov⁵⁵, G.R. Snow⁶⁷, J. Snow⁷⁴, S. Snyder⁷³, S. Söldner-Rembold⁴⁵, L. Sonnenschein²¹, A. Sopczak⁴³, M. Sosebee⁷⁸, K. Soustruznik⁹, B. Spurlock⁷⁸, J. Stark¹⁴, V. Stolin³⁸, D.A. Stoyanova⁴⁰, J. Strandberg⁶⁴, M.A. Strang⁶⁹, E. Strauss⁷², M. Strauss⁷⁵, R. Ströhmer²⁶, D. Strom⁵¹, L. Stutte⁵⁰, S. Sumowidagdo⁴⁹, P. Svoisky³⁶, M. Takahashi⁴⁵, A. Tanasijczuk¹, W. Taylor⁶, B. Tiller²⁶, M. Titov¹⁸, V.V. Tokmenin³⁷, I. Torchiani²³, D. Tsybychev⁷², B. Tuchming¹⁸, C. Tully⁶⁸, P.M. Tuts⁷⁰, R. Unalan⁶⁵, L. Uvarov⁴¹, S. Uvarov⁴¹, S. Uzunyan⁵², P.J. van den Berg³⁵, R. Van Kooten⁵⁴, W.M. van Leeuwen³⁵, N. Varelas⁵¹, E.W. Varnes⁴⁶, I.A. Vasilyev⁴⁰, P. Verdier²⁰, L.S. Vertogradov³⁷, M. Verzocchi⁵⁰, M. Vesterinen⁴⁵, D. Vilanova¹⁸, P. Vint⁴⁴, P. Vokac¹⁰, R. Wagner⁶⁸, H.D. Wahl⁴⁹, M.H.L.S. Wang⁷¹, J. Warchol⁵⁵, G. Watts⁸², M. Wayne⁵⁵, G. Weber²⁵, M. Weber^{50,g}, A. Wenger^{23,h}, M. Wetstein⁶¹, A. White⁷⁸, D. Wicke²⁵, M.R.J. Williams⁴³, G.W. Wilson⁵⁸, S.J. Wimpenny⁴⁸, M. Wobisch⁶⁰, D.R. Wood⁶³, T.R. Wyatt⁴⁵, Y. Xie⁷⁷, C. Xu⁶⁴, S. Yacoob⁵³, R. Yamada⁵⁰, W.-C. Yang⁴⁵, T. Yasuda⁵⁰, Y.A. Yatsunenkov³⁷, Z. Ye⁵⁰, H. Yin⁷, K. Yip⁷³, H.D. Yoo⁷⁷, S.W. Youn⁵⁰, J. Yu⁷⁸, C. Zeitnitz²⁷, S. Zelitch⁸¹, T. Zhao⁸², B. Zhou⁶⁴, J. Zhu⁷², M. Zielinski⁷¹, D. Zieminska⁵⁴, L. Zivkovic⁷⁰, V. Zutshi⁵², and E.G. Zverev³⁹

(The DØ Collaboration)

¹ Universidad de Buenos Aires, Buenos Aires, Argentina

² LAFEX, Centro Brasileiro de Pesquisas Físicas, Rio de Janeiro, Brazil

³ Universidade do Estado do Rio de Janeiro, Rio de Janeiro, Brazil

⁴ Universidade Federal do ABC, Santo André, Brazil

⁵ Instituto de Física Teórica, Universidade Estadual Paulista, São Paulo, Brazil

⁶ University of Alberta, Edmonton, Alberta, Canada; Simon Fraser University, Burnaby, British Columbia, Canada; York University, Toronto, Ontario, Canada and McGill University, Montreal, Quebec, Canada

⁷ University of Science and Technology of China, Hefei, People's Republic of China

⁸ Universidad de los Andes, Bogotá, Colombia

⁹ Center for Particle Physics, Charles University,

Faculty of Mathematics and Physics, Prague, Czech Republic

¹⁰ Czech Technical University in Prague, Prague, Czech Republic

¹¹ Center for Particle Physics, Institute of Physics,

Academy of Sciences of the Czech Republic, Prague, Czech Republic

¹² Universidad San Francisco de Quito, Quito, Ecuador

¹³ LPC, Université Blaise Pascal, CNRS/IN2P3, Clermont, France

¹⁴ LPSC, Université Joseph Fourier Grenoble 1, CNRS/IN2P3,

Institut National Polytechnique de Grenoble, Grenoble, France

¹⁵ CPPM, Aix-Marseille Université, CNRS/IN2P3, Marseille, France

¹⁶ LAL, Université Paris-Sud, IN2P3/CNRS, Orsay, France

¹⁷ LPNHE, IN2P3/CNRS, Universités Paris VI and VII, Paris, France

¹⁸ CEA, Irfu, SPP, Saclay, France

¹⁹ IPHC, Université de Strasbourg, CNRS/IN2P3, Strasbourg, France

²⁰ IPNL, Université Lyon 1, CNRS/IN2P3, Villeurbanne, France and Université de Lyon, Lyon, France

²¹ III. Physikalisches Institut A, RWTH Aachen University, Aachen, Germany

²² Physikalisches Institut, Universität Bonn, Bonn, Germany

²³ Physikalisches Institut, Universität Freiburg, Freiburg, Germany

²⁴ II. Physikalisches Institut, Georg-August-Universität Göttingen, Göttingen, Germany

²⁵ Institut für Physik, Universität Mainz, Mainz, Germany

²⁶ Ludwig-Maximilians-Universität München, München, Germany

²⁷ Fachbereich Physik, University of Wuppertal, Wuppertal, Germany

²⁸ Panjab University, Chandigarh, India

²⁹ Delhi University, Delhi, India

³⁰ Tata Institute of Fundamental Research, Mumbai, India

³¹ University College Dublin, Dublin, Ireland

³² Korea Detector Laboratory, Korea University, Seoul, Korea

³³ SungKyunKwan University, Suwon, Korea

³⁴ CINVESTAV, Mexico City, Mexico

³⁵ FOM-Institute NIKHEF and University of Amsterdam/NIKHEF, Amsterdam, The Netherlands

³⁶ Radboud University Nijmegen/NIKHEF, Nijmegen, The Netherlands

³⁷ Joint Institute for Nuclear Research, Dubna, Russia

- ³⁸*Institute for Theoretical and Experimental Physics, Moscow, Russia*
³⁹*Moscow State University, Moscow, Russia*
⁴⁰*Institute for High Energy Physics, Protvino, Russia*
⁴¹*Petersburg Nuclear Physics Institute, St. Petersburg, Russia*
⁴²*Stockholm University, Stockholm, Sweden, and Uppsala University, Uppsala, Sweden*
⁴³*Lancaster University, Lancaster, United Kingdom*
⁴⁴*Imperial College London, London SW7 2AZ, United Kingdom*
⁴⁵*The University of Manchester, Manchester M13 9PL, United Kingdom*
⁴⁶*University of Arizona, Tucson, Arizona 85721, USA*
⁴⁷*California State University, Fresno, California 93740, USA*
⁴⁸*University of California, Riverside, California 92521, USA*
⁴⁹*Florida State University, Tallahassee, Florida 32306, USA*
⁵⁰*Fermi National Accelerator Laboratory, Batavia, Illinois 60510, USA*
⁵¹*University of Illinois at Chicago, Chicago, Illinois 60607, USA*
⁵²*Northern Illinois University, DeKalb, Illinois 60115, USA*
⁵³*Northwestern University, Evanston, Illinois 60208, USA*
⁵⁴*Indiana University, Bloomington, Indiana 47405, USA*
⁵⁵*University of Notre Dame, Notre Dame, Indiana 46556, USA*
⁵⁶*Purdue University Calumet, Hammond, Indiana 46323, USA*
⁵⁷*Iowa State University, Ames, Iowa 50011, USA*
⁵⁸*University of Kansas, Lawrence, Kansas 66045, USA*
⁵⁹*Kansas State University, Manhattan, Kansas 66506, USA*
⁶⁰*Louisiana Tech University, Ruston, Louisiana 71272, USA*
⁶¹*University of Maryland, College Park, Maryland 20742, USA*
⁶²*Boston University, Boston, Massachusetts 02215, USA*
⁶³*Northeastern University, Boston, Massachusetts 02115, USA*
⁶⁴*University of Michigan, Ann Arbor, Michigan 48109, USA*
⁶⁵*Michigan State University, East Lansing, Michigan 48824, USA*
⁶⁶*University of Mississippi, University, Mississippi 38677, USA*
⁶⁷*University of Nebraska, Lincoln, Nebraska 68588, USA*
⁶⁸*Princeton University, Princeton, New Jersey 08544, USA*
⁶⁹*State University of New York, Buffalo, New York 14260, USA*
⁷⁰*Columbia University, New York, New York 10027, USA*
⁷¹*University of Rochester, Rochester, New York 14627, USA*
⁷²*State University of New York, Stony Brook, New York 11794, USA*
⁷³*Brookhaven National Laboratory, Upton, New York 11973, USA*
⁷⁴*Langston University, Langston, Oklahoma 73050, USA*
⁷⁵*University of Oklahoma, Norman, Oklahoma 73019, USA*
⁷⁶*Oklahoma State University, Stillwater, Oklahoma 74078, USA*
⁷⁷*Brown University, Providence, Rhode Island 02912, USA*
⁷⁸*University of Texas, Arlington, Texas 76019, USA*
⁷⁹*Southern Methodist University, Dallas, Texas 75275, USA*
⁸⁰*Rice University, Houston, Texas 77005, USA*
⁸¹*University of Virginia, Charlottesville, Virginia 22901, USA and*
⁸²*University of Washington, Seattle, Washington 98195, USA*

(Dated: December 4, 2009)

We report results from a search for production of a neutral Higgs boson in association with a b quark. We search for Higgs decays to τ pairs with one τ subsequently decaying to a muon and the other to hadrons. The data correspond to 2.7 fb^{-1} of $p\bar{p}$ collisions recorded by the D0 detector at $\sqrt{s} = 1.96 \text{ TeV}$. The data are found to be consistent with background predictions. The result allows us to exclude a significant region of parameter space of the minimal supersymmetric model.

PACS numbers: 14.80.Da, 13.85.Rm, 12.60.Jv

The current model of physics at high energies, the standard model (SM), has withstood increasingly precise experimental tests, although the Higgs boson needed to mediate the breaking of electroweak symmetry [1] has not been found. Despite the success of the SM, it has several shortcomings. Theories invoking a new fermion-boson symmetry, called supersymmetry [2] (SUSY), provide an

attractive means to address the hierarchy problem, non-unification of couplings at high energy, and offer a dark matter candidate. In addition to new SUSY-specific partners to SM particles, these theories have an extended Higgs sector. In the minimal supersymmetric standard model (MSSM) there are two Higgs doublet fields which result in five physical Higgs bosons: two neutral scalars

(h, H), a neutral pseudoscalar (A) and two charged Higgs bosons (H^\pm). The mass spectrum of the Higgs bosons is determined at tree level by two parameters, typically chosen to be $\tan\beta$, the ratio of the vacuum expectation values of up-type and down-type scalar fields and M_A , the mass of the physical pseudoscalar. Higher order corrections to the masses and couplings are dominated by the Higgsino mass parameter μ and the mixing of scalar top quarks.

In this Letter, we present a search for neutral Higgs bosons (collectively denoted ϕ) produced in association with a b quark. The specific Higgs boson decay mode used in this search is $\phi \rightarrow \tau\tau$ with one of the τ leptons subsequently decaying via $\tau \rightarrow \mu\nu_\tau\nu_\mu$ (denoted τ_μ) and the second via $\tau \rightarrow \text{hadrons} + \nu_\tau$ (denoted τ_h). In the MSSM the A coupling to down-type fermions is enhanced by a factor $\propto \tan\beta$ and thus the Higgs production cross section is enhanced by a factor $\propto \tan^2\beta$ relative to the SM, giving potentially detectable rates at the Tevatron. Two of the three neutral Higgs bosons have nearly degenerate masses over much of the parameter space, effectively giving another factor of two in production rate. A previous search in this final state was carried out by the D0 experiment [3]. Searches in the complementary channels $\phi Z/\phi\phi \rightarrow b\bar{b}\tau\tau, \tau\tau b\bar{b}$ [4], $\phi \rightarrow \tau\tau$ [5, 6], and $\phi b \rightarrow b\bar{b}b$ [7, 8] have also been carried out by the LEP, D0, and CDF experiments. By searching in complementary channels we reduce overall sensitivity to the particular details of the model. The $b\tau\tau$ final state is less sensitive to SUSY radiative corrections than the $b\bar{b}b$ final state, and has greater sensitivity at low Higgs mass than the $\phi \rightarrow \tau\tau$ channel, as the b -jet in the final state reduces the $Z \rightarrow \tau\tau$ background. Furthermore, an additional complementary channel will contribute to an even stronger exclusion when combining different searches. The result presented in this Letter uses an integrated luminosity of 2.7 fb^{-1} which is eight times that used for the previous result in this channel. Because of analysis improvements, the gain in sensitivity compared to the prior result is greater than expected from the increased integrated luminosity only. We also extend the Higgs mass search range relative to the previous result in this channel.

The D0 detector [9] is a general purpose detector located at Fermilab's Tevatron $p\bar{p}$ collider. The Tevatron operates at a center of mass energy of 1.96 TeV. This analysis relies on all aspects of the detector: tracking, calorimetry, muon detection, the ability to identify detached vertices and the luminosity measurement.

This search requires reconstruction of muons, hadronic τ decays, jets (arising from b quarks) and neutrinos. Muons are identified using track segments in the muon system and are required to have a track reconstructed in the inner tracking system which is close to the muon-system track segment in η and φ . Here η is the pseudorapidity and φ is the azimuthal angle in the plane perpendicular to the beam. Jets are reconstructed from

calorimeter information using the D0 Run II cone algorithm [10] with a radius of $R = 0.5$ in (y, φ) space, where $R = \sqrt{(\Delta y)^2 + \Delta\varphi^2}$ and y is the rapidity. Jets are additionally identified as being consistent with decay of a b -flavored hadron (b -tagged) if the tracks aligned with the calorimeter jet have high impact parameter or form a vertex separated from the primary interaction point in the plane transverse to the beam as determined by a neural network (NN_b) algorithm [11]. Hadronic τ decays are identified [12] as clusters of energy in the calorimeter reconstructed [10] using a cone algorithm of radius $R = 0.3$ which have associated tracks. The τ candidates are then categorized as being one of three types which correspond roughly to one-prong τ decay with no π^0 s (called Type 1), one-prong decay with π^0 s (Type 2) and multiprong decay (Type 3). A final identification requirement is based on the output value of a neural network (NN_τ) designed to separate τ leptons from jets. The missing transverse energy \cancel{E}_T is used to infer the presence of neutrinos. The \cancel{E}_T is the negative of the vector sum of the transverse energy of calorimeter cells satisfying $|\eta| < 3.2$. We correct the \cancel{E}_T for the energy scales of reconstructed final state objects, including muons.

Signal acceptance and efficiency are modeled using simulated SM ϕb events generated with the PYTHIA event generator [13] requiring the b quark to satisfy $p_T > 15 \text{ GeV}/c$ and $|\eta| < 2.5$ and using the CTEQ6L1 [14] parton distribution functions (PDF). The TAUOLA [15] program is used to model τ decay and EVTGEN [16] is used to decay b hadrons. The dependence of the Higgs boson decay width on $\tan\beta$ is included by reweighting PYTHIA samples, and the kinematic properties are reweighted to the prediction of the NLO program MCFM [17]. The generator outputs are passed through a detailed detector simulation based on GEANT [18]. Each GEANT event is combined with collider data events recorded during a random beam crossing to model the effects of detector noise, pileup, and additional $p\bar{p}$ interactions. The combined output is then passed to the D0 event reconstruction program. Simulated signal samples are generated for different Higgs masses ranging from 90 to $320 \text{ GeV}/c^2$.

Backgrounds to this search are dominated by Z +jets, $t\bar{t}$, and multijet (MJ) production. In the MJ background the apparent leptons primarily come from semileptonic b hadron decays, not τ decays. Additional backgrounds include W +jets events, SM diboson production and single top quark production. Except for the MJ contribution, all background yields are estimated using simulated events, with the same processing chain used for signal events. The Z +jets, W +jets and $t\bar{t}$ samples are generated using ALPGEN [19] with PYTHIA used for fragmentation. The diboson samples are generated using PYTHIA. For simulated samples in which there is only one lepton arising from the decay of a W boson or from $t\bar{t} \rightarrow \ell$ +jets, the second lepton is either a jet misidentified as a τ or a muon+jet system from heavy flavor decay in which the

muon is misidentified as being isolated from other activity.

Corrections accounting for differences between data and the simulation are applied to the simulated events. The corrections are derived from control data samples and applied to object identification efficiencies, trigger efficiencies, primary $p\bar{p}$ interaction position (primary vertex) and the transverse momentum spectrum of Z bosons. After applying all corrections, the yields for signal and each background are calculated as the product of the acceptance times efficiency determined from simulation, luminosity and predicted cross sections.

The initial analysis step is selection of events recorded by at least one trigger from a set of single muon triggers for data taken before the summer of 2006. For data taken after summer 2006 we require at least one trigger from a set of single muon triggers and muon plus hadronic τ triggers. The average trigger efficiency for signal events is approximately 65% for both data epochs.

After making the trigger requirements a background-dominated pre-tag sample is selected by requiring a reconstructed primary vertex for the event with at least three tracks, exactly one reconstructed hadronic τ , exactly one isolated muon, and at least one jet. This analysis requires the τ candidates to satisfy $E_T^\tau > 10$ GeV, $p_T^\tau > 7(5)$ GeV/ c and $NN_\tau > 0.9$ for Type 1(2) taus, $E_T^\tau > 15$ GeV, $p_T^\tau > 10$ GeV/ c and $NN_\tau > 0.95$ for Type 3 taus. Here E_T^τ is the transverse energy of the τ measured in the calorimeter, p_T^τ is the transverse momentum sum of the associated track(s). These NN_τ requirements have an efficiency of $\approx 65\%$ in signal events and a misclassification probability of $\approx 1\%$ in multijet events. The muon must satisfy $p_T^\mu > 12$ GeV/ c and $|\eta| < 2.0$. It is also required to be isolated from activity in the tracker and calorimeter [20]. Selected jets have $E_T > 15$ GeV, $|\eta| < 2.5$. The τ , the muon and jets must all be consistent with arising from the same primary vertex and be separated from each other by $\Delta R > 0.5$. In addition, the muon and τ are required to have opposite charge, and the (μ, \cancel{E}_T) mass variable $M \equiv \sqrt{2\cancel{E}_T E_\mu^2 / p_T^\mu (1 - \cos(\Delta\varphi(\mu, \cancel{E}_T)))}$ must satisfy $M < 80, < 80, < 60$ GeV/ c^2 for events with τ s of Type 1, 2 and 3 respectively. Here E_μ is the energy of the muon, and $\Delta\varphi$ is the opening angle between the \cancel{E}_T and muon in the plane transverse to the beam direction.

A more restrictive b -tag subsample with improved signal to background ratio is defined by demanding that at least one jet in each event is consistent with b quark production [11]. The b -jet identification efficiency in signal events is about 35% and the probability to misidentify a light jet as a b jet is 0.5%. Approximately 94% of the b -tag sample has at least one true heavy flavor jet.

All backgrounds except MJ are derived from simulated events as described earlier. The MJ background is derived from control data samples. A parent MJ-enriched

control sample is created by requiring a muon, τ , and jet as above, but with the muon isolation requirement removed and with a lower quality ($0.3 \leq NN_\tau \leq 0.9$) τ selected. This is then used to create a b -tag subsample which requires at least one of the jets to be identified as a b jet with the same b jet selection as earlier. The residual contributions from SM backgrounds are subtracted from the MJ control samples using simulated events.

To determine the MJ contribution in the pre-tag analysis sample, a data sample is used that has the same selection as the pre-tag analysis sample except that the muon and τ charges have the same sign. This same-sign (SS) sample is dominated by MJ events. After making a subtraction of other SM background processes which contribute to this sample, the number of MJ events in the opposite-sign (OS) signal region is computed by multiplying the SS sample by the OS/SS ratio, 1.05 ± 0.02 , determined in a control sample selected by requiring a non-isolated muon.

For the b -tag analysis sample, statistical limitations require a different approach for the MJ background evaluation than for the pre-tag sample. For the b -tag sample, two methods are used. For the first method, the per jet probability P_{tag} that a jet in the SS MJ control subsample would be identified as a b jet is determined as a function of jet p_T . We apply P_{tag} to the jets in the SS pre-tag sample to determine the yield in the b -tag sample. For the second method, the MJ background is determined by multiplying the b -tag MJ control sample yield by two factors: (1) the probability that the non-isolated muon would be identified as isolated, and (2) the ratio of events with a τ candidate passing the NN_τ requirements to events with τ candidates having $0.3 \leq NN_\tau < 0.9$ as determined in a separate control sample. The final MJ contribution in the b -tag analysis sample is determined using the MJ shape from the first method with the normalization equal to the average of the two methods. We include the normalization difference between the two methods in the systematic uncertainty on the MJ contribution.

The signal to background ratio is further improved using multivariate techniques. Two separate methods are used, one to address the $t\bar{t}$ background and one to reduce the MJ background. For the $t\bar{t}$ background, a neural network (NN_{top}) is constructed using $H_T \equiv \sum_{jets} E_T$, $E_{tot} \equiv \sum_{jets} E + E_\tau + E_\mu$, the number of jets and $\Delta\varphi(\mu, \tau)$ as inputs. For the MJ background, a simple joint likelihood discriminant (LL_{MJ}) is constructed using p_T^μ , p_T^τ , $\Delta R(\mu, \tau)$, $M_{\mu\tau}$ and $M_{\mu\tau\nu}$. Here $M_{\mu\tau}$ denotes the invariant mass of the muon and tau, and $M_{\mu\tau\nu}$ is the invariant mass computed from the muon, τ , and \cancel{E}_T momentum vectors. The final analysis sample is defined by selecting rectangular regions in the NN_{top} versus LL_{MJ} plane. The regions have been identified for each τ type and each Higgs boson mass point separately by optimizing the search sensitivity using simulated events. The signal

	Pre-tag	b -tagged	Final
$t\bar{t}$	66.0 ± 1.3	39.6 ± 0.8	20.3 ± 0.6
Multijet	549 ± 26	38.5 ± 2.3	28.1 ± 1.9
$Z(\rightarrow \tau\tau) + \text{jets}$	1241 ± 8	18.8 ± 0.3	16.3 ± 0.3
Other Bkg	267 ± 6	5.1 ± 0.1	4.1 ± 0.1
Total Bkg	2123 ± 28	102 ± 2.4	68.7 ± 2.0
Data	2077	112	79
Signal	26.5 ± 0.3	8.8 ± 0.1	8.4 ± 0.1

TABLE I: Predicted background yield, observed data yield and predicted signal yield and their statistical uncertainties at three stages of the analysis. The signal yields are based on the sum of all neutral Higgs bosons assuming $\tan\beta = 40$ and $M_A = 120 \text{ GeV}/c^2$ for the m_h^{max} and $\mu = -200 \text{ GeV}/c^2$ scenario. The total background uncertainty at the Final analysis stage including systematic uncertainties is 8.4 events.

to background ratio improves by up to a factor of two when applying these requirements.

Table I shows the predicted background and observed data yields in the analysis samples. The selection efficiency for signal events varies between 5% and 10% depending on M_ϕ .

Systematic uncertainties arise from a variety of sources. Most are evaluated using comparisons between data control samples and predictions from simulation. The uncertainties are divided into two categories: (1) those which affect only normalization, and (2) those which also affect the shape of distributions. The sources in the first category include the luminosity (6.1%), muon identification efficiency (4.5%), τ_h identification (5%, 4%, 8%), τ_h energy calibration (3%), the $t\bar{t}$ and single top cross sections (11% and 12%), diboson cross sections (6%), $Z+(u,d,s,c)$ rate (+2%, -5%) and the $W + b$ and $Z + b$ cross sections (30%); those in the second include jet energy calibration (2%-4%), b -tagging (3%-5%), trigger (3%-5%), and MJ background (33%, 12%, 11%). For sources with three values, the values correspond to τ Types 1, 2 and 3 respectively.

After making the final selection, the discriminant D is formed from the product of the NN_{top} and LL_{MJ} variables, $D = LL_{MJ} \times NN_{top}$. The resulting distributions for the predicted background, signal and data are shown in Fig. 1(a). This distribution is used as input to a significance calculation using a modified frequentist approach with a Poisson log-likelihood ratio test statistic [21]. In the absence of a significant signal we set 95% confidence level limits on the presence of neutral Higgs bosons in our data sample. The cross section limits are shown in Fig. 1(b) as a function of Higgs boson mass. We translate them into the $\tan\beta$ versus M_A plane in several MSSM benchmark scenarios [22–24], including the $m_h^{max}, \mu = -200 \text{ GeV}/c^2$ scenario shown in Fig. 1(c). Results for other scenarios are in [25]. The signal cross sections and branching fractions are computed using FEYNHIGGS [26]. Instabilities in the theoretical cal-

culational for $\tan\beta > 100$ limit the usable mass range in the translation into the $(\tan\beta, M_A)$ plane.

In summary, this Letter reports a search for production of Higgs bosons in association with a b quark using eight times more data than previous results for this channel. The data are consistent with predictions from known physics sources and limits are set on the neutral Higgs boson associated production cross section. These cross section limits, a factor of three improvement over previous results, are also translated into limits in the SUSY parameter space.

We thank the staffs at Fermilab and collaborating institutions, and acknowledge support from the DOE and NSF (USA); CEA and CNRS/IN2P3 (France); FASI, Rosatom and RFBR (Russia); CNPq, FAPERJ, FAPESP and FUNDUNESP (Brazil); DAE and DST (India); Colciencias (Colombia); CONACyT (Mexico); KRF and KOSEF (Korea); CONICET and UBACyT (Argentina); FOM (The Netherlands); STFC and the Royal Society (United Kingdom); MSMT and GACR (Czech Republic); CRC Program, CFI, NSERC and WestGrid Project (Canada); BMBF and DFG (Germany); SFI (Ireland); The Swedish Research Council (Sweden); and CAS and CNSF (China).

-
- [a] Visitor from Augustana College, Sioux Falls, SD, USA.
 - [b] Visitor from Rutgers University, Piscataway, NJ, USA.
 - [c] Visitor from The University of Liverpool, Liverpool, UK.
 - [d] Visitor from SLAC, Menlo Park, CA, USA.
 - [e] Visitor from Centro de Investigacion en Computacion - IPN, Mexico City, Mexico.
 - [f] Visitor from ECFM, Universidad Autonoma de Sinaloa, Culiacán, Mexico.
 - [g] Visitor from Universität Bern, Bern, Switzerland.
 - [h] Visitor from Universität Zürich, Zürich, Switzerland.
- [1] A. Djouadi, Phys. Rep. **457**, 1 (2008); A. Djouadi, Phys. Rep. **459**, 1 (2008); and references therein.
 - [2] H. P. Nilles, Phys. Rep. **110**, 1 (1984); H. E. Haber and G. L. Kane, Phys. Rep. **117**, 75 (1985).
 - [3] V.M. Abazov *et al.* (D0 Collaboration), Phys. Rev. Lett. **102**, 051804 (2009).
 - [4] The LEP Working Group for Higgs Boson Searches (ALEPH, DELPHI, L3, and OPAL Collaborations), Eur. Phys. J. C **47**, 547 (2006).
 - [5] V.M. Abazov *et al.* (D0 Collaboration), Phys. Rev. Lett. **101**, 071804 (2008).
 - [6] A. Abulencia *et al.* (CDF Collaboration), Phys. Rev. Lett. **96**, 011802 (2006).
 - [7] V.M. Abazov *et al.* (D0 Collaboration), Phys. Rev. Lett. **101**, 221802 (2008).
 - [8] T. Affolder *et al.* (CDF Collaboration), Phys. Rev. Lett. **86**, 4472 (2001).
 - [9] V.M. Abazov *et al.* (D0 Collaboration), Nucl. Instrum. Methods in Phys. Res. A **565**, 463 (2006).
 - [10] G. Blazey *et al.*, arXiv:hep-ex/0005012 (2000).
 - [11] V.M. Abazov *et al.* (D0 Collaboration), arXiv:1002.4224

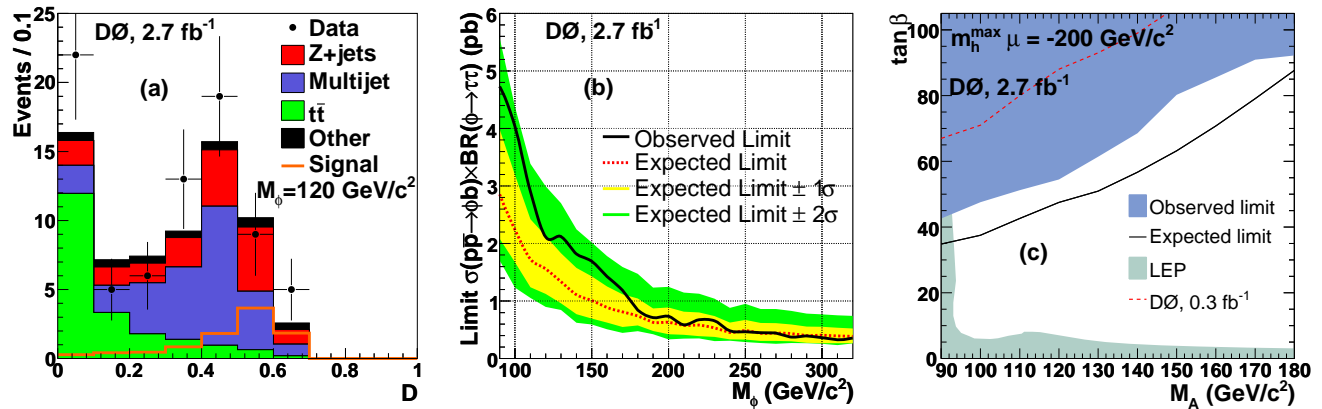


FIG. 1: (a) The distribution of the final discriminant variable, $D = NN_{top} \times LL_{MJ}$. The figure includes all τ Types. (b) The cross-section limit as a function of Higgs boson mass. (c) The region in the $\tan\beta$ versus M_A plane excluded by this analysis, LEP neutral MSSM Higgs searches, and the previous D0 result in this channel.

- [hep-ex], to be published in Nucl. Instrum. Methods in Phys. Res. **A**.
- [12] V.M. Abazov *et al.* (D0 Collaboration), Phys. Lett. B **670**, 292 (2009).
- [13] T. Sjöstrand *et al.*, Comput. Phys. Commun. **135**, 238 (2001). Version 6.409.
- [14] J. Pumplin *et al.*, JHEP **0207**, 012 (2002); D. Stump *et al.*, JHEP **0310**, 046 (2003).
- [15] Z. Was, Nucl. Phys. B - Proc. Suppl. **98**, 96 (2001). Version 2.5.04.
- [16] D.J. Lange, Nucl. Instrum. Methods in Phys. Res. A **462**, 152 (2001). Version 9.39.
- [17] J. Campbell and R.K. Ellis, Phys. Rev. D **65**, 113007 (2002). Version 5.6.
- [18] R. Brun and F. Carminati, CERN Program Library Long Writeup W5013, 1993 (unpublished). Version 3.21.
- [19] M.L. Mangano, M. Moretti, F. Piccinini, R. Pittau, and A. Polosa, JHEP **07**, 001 (2003). Version 2.11.
- [20] V.M. Abazov *et al.* (D0 Collaboration), Phys. Rev. Lett. **93**, 141801 (2004).
- [21] W. Fisher, FERMILAB-TM-2386-E (2007).
- [22] M. Carena, S. Heinemeyer, C.E.M. Wagner, G. Weiglein, Eur. Phys. J. C **45**, 797 (2006).
- [23] M. Carena, S. Heinemeyer, C.E.M. Wagner, G. Weiglein, Eur. Phys. J. C **26**, 601 (2003).
- [24] S. Heinemeyer, W. Hollik, G. Weiglein, JHEP **6**, 009 (2000).
- [25] See <http://link.aps.org/supplemental/xxx> for additional tables and figures including results for other MSSM benchmark scenarios.
- [26] M. Frank, T. Hahn, S. Heinemeyer, W. Hollik, H. Rzehak, and G. Weiglein, JHEP **0702**, 47 (2007). Version 2.6.5; G. Degrossi, S. Heinemeyer, W. Hollik, P. Slavich, G. Weiglein, Eur. Phys. J. C **28**, 133 (2003); S. Heinemeyer, W. Hollik, G. Weiglein, Eur. Phys. J. C **9**, 343 (1999); S. Heinemeyer, W. Hollik, G. Weiglein, Comput. Phys. Commun. **124**, 76 (2000).